High-contrast imaging of graphene via time-domain terahertz spectroscopy

J.L. Tomaino,[1] A.D. Jameson,[1] M.J. Paul,[1] J.W. Kevek,[2] A.M. van der Zande,[2] R.A. Barton,[3] H. Choi,[4] P.L. McEuen,[2,5] E.D. Minot,[1] and Yun-Shik Lee[1,*]

[1]Department of Physics, Oregon State University, Corvallis, Oregon 97331-6507, USA

[2]Laboratory of Atomic and Solid-State Physics, Cornell University, Ithaca, NY 14853, USA

[3]School of Applied and Engineering Physics, Cornell University, Ithaca, NY 14853, USA

[4]School of Electrical and Electronic Engineering, Yonsei University, Seoul, Republic of Korea

[5]Kavli Institute at Cornell for Nanoscale Science, Cornell University, Ithaca, NY 14853, USA

Corresponding author: Yun-Shik Lee

E-mail) leeys@physics.oregonstate.edu

Tel) 541-737-5057

Fax) 54-737-16834

Abstract

We demonstrate terahertz (THz) imaging and spectroscopy of single-layer graphene deposited on an intrinsic Si substrate using THz time-domain spectroscopy. A single-cycle THz pulse undergoes multiple internal reflections within the Si substrate, and the THz absorption by the graphene layer accumulates through the multiple interactions with the graphene/Si interface. We exploit the large absorption of the multiply reflected THz pulses to acquire high-contrast THz images of graphene. We obtain local sheet conductivity of the graphene layer analyzing the transmission data with thin-film Fresnel formula based on the Drude model.

Keywords

Graphene; Terahertz Imaging; Time-Domain Spectroscopy; Multiple Internal Reflections

1. Introduction

Recent advances in graphene fabrication [1-4] have opened up new opportunities for carbon-based electronics. Its applications are broad, ranging from ultra-high speed microelectronics [5,6] to large-size touch screens [7]. The new class of the opto-electronic applications exploits the unique electrical and optical properties of graphene, arising from the linear dispersion of the energy band, such as ballistic nature of charge transport [8], massless relativistic electrons [9], and the coexistence of conductivity and transparency [10,11]. An important stepping stone for realizing graphene devices is, therefore, to understand the charge carrier transport across a graphene layer. It is challenging to acquire a comprehensive transport picture of graphene. The typical electrical characterization using metal contacts provides limited information to understand the nature of charge transport because of the unavoidable contact artifacts on the one-atom layer of graphene and inflicts permanent damage upon the material. Terahertz (THz) spectroscopy provides a *non-contact electrical probe*, and hence circumvents many constraints of the conventional measurement techniques [12]. THz spectroscopy of epitaxial graphene on SiC has shown that the carrier scattering time is estimated as ~2 fs [13]. It was recently demonstrated that THz imaging and spectroscopy of a large-area, single-layer graphene film clearly mapped out the THz carrier dynamics of the graphene and measured the sheet conductivity with sub-mm resolution without fabricating electrodes [14].

In this paper, we present THz imaging of single-layer graphene using THz time-domain spectroscopy (THz-TDS). The graphene sample was grown on Cu-foil and subsequently transferred to a Si substrate. We have measured the transmission of broadband THz pulses through the graphene-on-Si sample. A THz pulse undergoes multiple internal reflections within the Si substrates, and the THz pulse absorption accumulates through the multiple interactions with the graphene/Si interface. We exploit the strong absorption of the multiply reflected THz pulses to acquire high-contrast images of the graphene-on-Si sample. Using the THz absorption data, we determine the local sheet conductivity of the graphene layer.

2. Terahertz Time-Domain Spectroscopy of Graphene-on-Si

We grew graphene using the method of chemical vapor deposition (CVD) on Cu foil [3]. A mixture of methane (158 sccm) and hydrogen (6 sccm) passes by a Cu substrate (Alfa Aesar, 25-μm thickness) flowing through a one-inch tube furnace. The substrate temperature maintained at 1000°C, and the pressure of the CVD system was reduced to 5.5 Torr to keep the graphene growth to single layer. We transferred the graphene film to an intrinsic Si substrate via the following procedure: (i) coat the surface of the graphene-on-Cu with PMMA (500-nm thickness), (ii) remove the Cu foil by etching in a $FeCl_3$-based solution (CE-200, Transene), (iii) wash the PMMP-graphene film with DI water, (iv) lift up the PMMA-graphene film using the Si substrate, and (iv) remove the PMMA by soaking in methylene chloride. We used the intrinsic Si substrate because of its exceptionally low absorption in the THz region. Micro-Raman spectroscopy of the graphene-on-Si sample confirmed that the graphene is predominately single-layer with low disorder as shown in the inset of Fig. 1 [15]. The position of the G-peak (1589 cm^{-1}) indicates that the hole density is ~4 x 10^{12} cm^{-2} [16]. Extensive characterization of control samples by micro-Raman spectroscopy and scanning electron microscopy verified that the growth method produces > 90% coverage of single layer graphene.

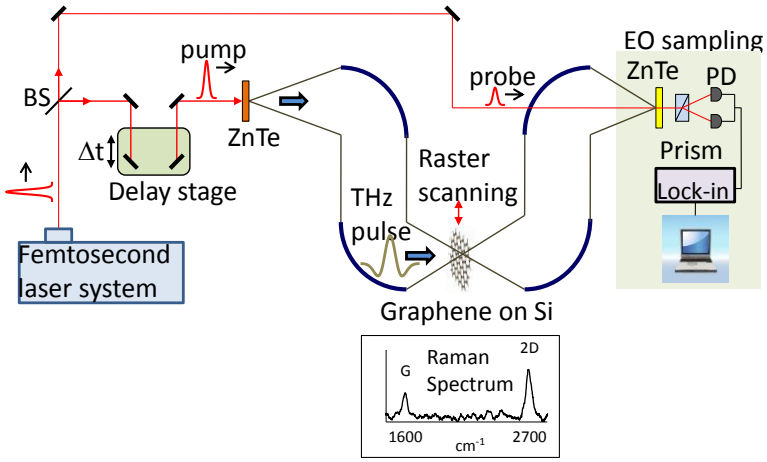

Fig. 1. Two-dimensional raster-scan imaging with broadband THz pulses in transmission geometry. Transmitted THz waveforms are measured by EO sampling. The inset at the bottom shows the Raman spectrum of the graphene sample

We carried out THz transmission imaging of the graphene sample by two-dimensional raster scanning with broadband THz pulses. Figure 1 illustrates the experimental set up of the THz time-domain spectroscopy in the transmission geometry. We generated the broadband THz pulses by optical rectification of femtosecond laser pulses (pulse energy, 1 mJ; pulse duration, 90 fs) in a 1-mm ZnTe crystal. The THz spectrum was centered at 1 THz and its bandwidth was 1.5 THz. The graphene sample was placed at the focus of the THz beam (beam diameter, 0.5 mm). We obtained the transmitted THz waveforms measuring the time-resolved THz-field amplitude by electro-optic (EO) sampling in a 1-mm ZnTe crystal.

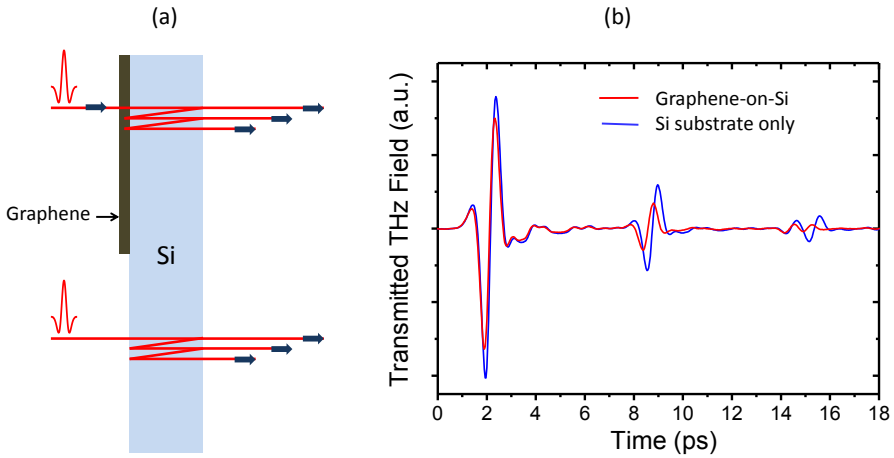

Fig. 2. THz pulses transmitted through the graphene-on Si sample and the Si substrate.

When a THz pulse enters into the graphene-on-Si sample, a portion of the pulse is directly transmitted while the rest undergoes multiple internal reflections at the front and back interfaces of the Si substrate before being transmitted to the detection setup (Fig. 2a). Since the Si substrate is substantially thicker (285±5 μm) than the THz pulse length in Si (~85 μm), the reflected pulses are temporally well separated from each other. Figure 2(b) shows the THz waveforms transmitted through the graphene-on-Si sample (red) and the Si substrate (blue). The waveforms are composed of a directly transmitted pulse and the subsequent "echos" corresponding to the multiple reflections

from the front and back sides of the Si substrate. The time delay between echoes (6.6 ps) is consistent with the roundabout optical path length in the Si substrate (substrate thickness, 285 μm; refractive index of Si at THz frequencies, 3.42). Because a large portion of the reflected THz pulses are absorbed by the graphene/Si interface, the amplitude of the echos through the graphene-on-Si sample decay much faster than that of the bare Si substrate.

We obtained the sheet conductivity of the graphene sample using the transmission measurements. We analyzed the data employing thin-film Fresnel coefficients based on the Drude model. The graphene-on-Si sample consisted of four layers (air-Graphene-Si-air). The graphene was treated as an infinitely thin film while the Si was treated as a lossless, thick optical medium. The transmission coefficient through the first interface (air→graphene→Si) is given by

$$t(\sigma_S) = \frac{2}{n_{Si} + 1 + Z_0\sigma_S} \tag{1}$$

and the internal reflection coefficient of the graphene/Si interface is given by

$$r(\sigma_S) = \frac{n_{Si} - 1 - Z_0\sigma_S}{n_{Si} + 1 + Z_0\sigma_S} \tag{2}$$

where n_{Si} is the refractive index of Si , σ_s is the sheet conductivity of graphene, and Z_0 (376.7 Ω) is the vacuum impedance. The transmission coefficient for the *m*-th pulse is therefore

$$\text{Graphene-on-Si:}\quad t_m = t \cdot (r_{34} \cdot r)^{m-1} \cdot t_{34} \cdot e^{i(2m-1)\phi_S} \tag{3}$$

$$\text{Si substrate only:}\quad t_{Si,m} = t_{13} \cdot (r_{34} \cdot r_{31})^{m-1} \cdot t_{34} \cdot e^{i(2m-1)\phi_S} \tag{4}$$

where $t_{ij} = 2n_i/(n_i + n_J)$ and $r_{ij} = (n_i - n_j)/(n_i + n_j)$ are the Fresnel coefficients with the refractive indices $n_1 = n_4 = n_{\text{air}} = 1$ and $n_3 = n_{Si} = 3.42$ and ϕ_S is the phase acquired while propagating through the Si substrate. The relative transmission for the *m*-th pulse is then

$$t_R^{(m)} = \frac{t_m}{t_{Si,m}} = \frac{t}{t_{13}}\left(\frac{r}{r_{31}}\right)^{m-1} \tag{5}$$

The average relative transmission of the directly transmitted pulses (*m*=1) over the entire graphene sample is 85.6%, which leads to a sheet conductivity σ_s=1.96×10^{-3} Ω^{-1}. This result agrees very well with our previous work (σ_s=2.04×10^{-3} Ω^{-1}), where we used a Si:Bolometer to measure the transmitted THz power through the sample [14].

3. Terahertz Imaging with Multiply Reflected Pulses

We exploit the high contrast of the second pulse ($t_R^{(2)} = 0.454$ in the TDS measurements) to construct 2-D graphene images using the time-resolved waveforms. We collected 750 second-pulses for a 25×20-mm^2 area with 1-mm pixels. The rich information contained in the time-resolved data provides many different display options to construct THz-TDS images.

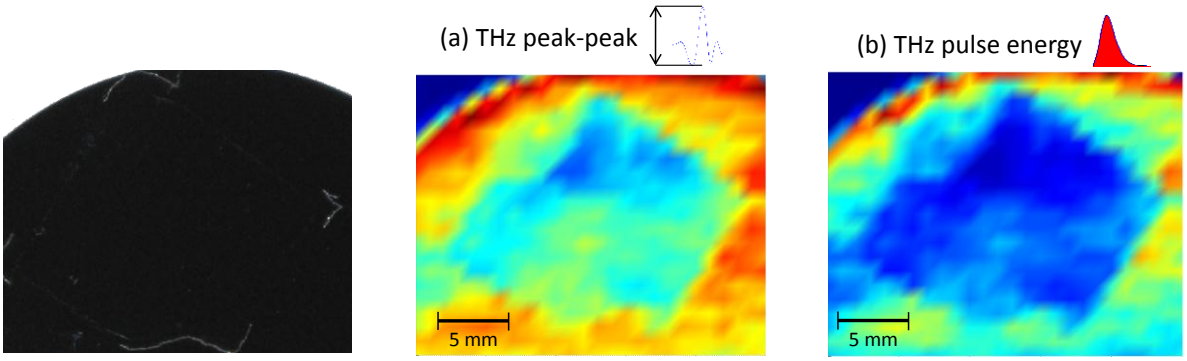

Fig. 3. THz-TDS images of graphene: (a) peak-to-peak field-amplitude image (b) pulse-energy image. A photograph of the graphene-on-Si sample is included for comparison.

The images in Fig. 3 are constructed (a) by the peak-to-peak values of the THz waveforms and (b) by the transmitted pulse energies. The dark square shape (~1.5×1.5 cm^2) in the figures indicates the graphene layer sitting on the Si substrate. The pulse-energy image shows higher contrast than the field-amplitude image. We also plotted images using the transmission spectra. We include an optical photograph of the sample for comparison. The white markers indicate the square-shape area where the graphene sheet is located, yet it is hardly discernible.

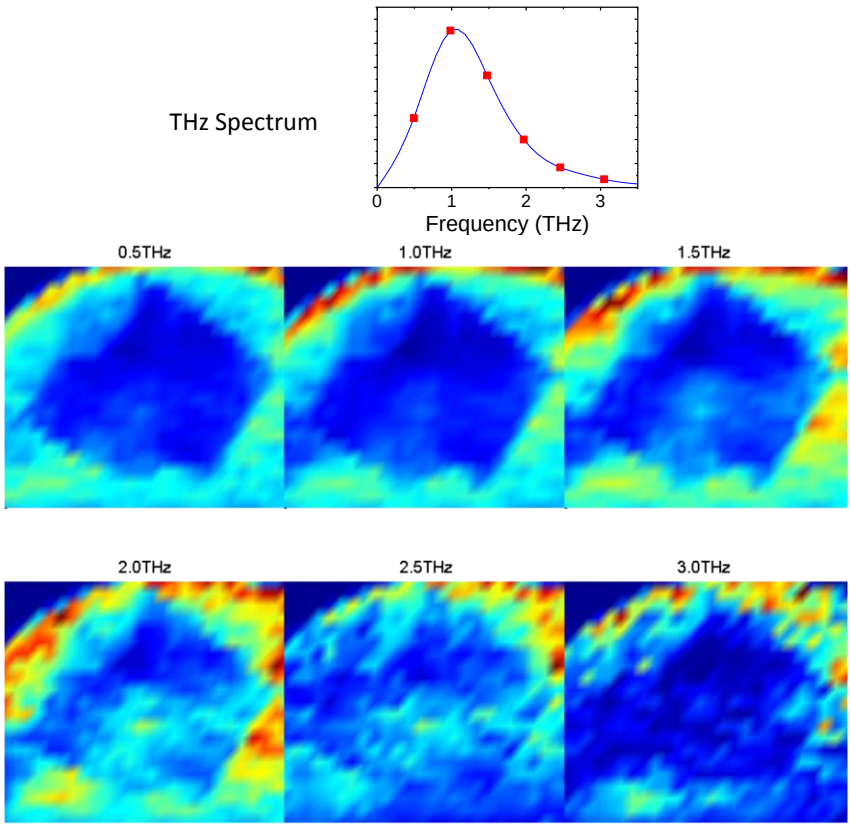

Fig. 4. THz transmission images of graphene at 0.5, 1.0, 1.5, 2.0, 2.5, and 3.0 THz

Figure 4 shows THz transmission images at different frequencies from 0.5 to 3.0 THz. Comparing them with Fig. 6(b), one can see that the spectral imaging is effective over the broad range where the spectral density of the THz pulse is relatively strong (0.5-1.5 THz). The signal-to-noise ratio quickly falls off outside of this range. Overall, the THz-TDS images show that the graphene conductivity is not spatially uniform. It is ~5% higher in the top-right corner than other regions.

5. Conclusion

Using THz-TDS we acquired high-contrast images of single-layer graphene and its local sheet conductivity (σ_s=1.96×10^{-3} Ω^{-1}). This method has several advantages over traditional electric probe techniques. It is a non-contacting probe as no physical probes are required to examine the electrical properties of the sample. It measures conductivity in a localized area and is therefore not affected by neighboring defects. The rich information contained in the time-resolved data provides multiple ways to demonstrate the electrical and optical properties of graphene at THz frequencies.

Acknowledgement

The work at Oregon State University was supported by Oregon Nanoscience and Microtechnologies Institute, National Science Foundation (DMR-1063632), and National Research Foundation (NRF) of Korea Grant funded by the Korean Government (NRF-2011-220-D00052) which also supported the work at the Yonsei University. The work at the Yonsei University was supported by the Basic Research Program through the NRF of Korea funded by the Ministry of Education, Science, and Technology (2011-0013255). The work at Cornell was supported by the NSF through the Cornell Center for Materials Research (CCMR), the MARCO Focused Research Center on Materials, Structures, and Devices and the AFOSR. Sample Fabrication was performed at the Cornell node of the National Nanofabrication Infrastructure Network, which is supported by the National Science Foundation (Grant ECS-0335765).

References

1. Berger, Z. Song, X. Li, X. Wu, N. Brown, C. Naud, D. Mayou, T. Li, J. Hass, A. N. Marchenkov, E. H. Conrad, P. N. First, and W. A. de Heer, "Electronic confinement and Coherence in Patterned Epitaxial Grahene," Science **312**, 1191-1196 (2006).
2. Keun Soo Kim, Yue Zhao, Houk Jang, Sang Yoon Lee, Jong Min Kim, Kwang S. Kim, Jong-Hyun Ahn, Philip Kim, Jae-Young Choi, and Byung Hee Hong, "Large-scale pattern growth of graphene films for stretchable transparent electrodes," Nature **457**, 706-710 (2009).
3. X. Li , W. Cai, J. An, S. Kim, J. Nah, D. Yang, R. Piner, A. Velamakanni, I. Jung, E. Tutuc, S. K. Banerjee, L. Colombo, and R. S. Ruoff, **"**Large-area synthesis of high-quality and uniform graphene films on copper foils," Science **324**(5932), 1312-1314 (2009).
4. Y. Lee, S. Bae, H. Jang, S. Jang, S.-E. Zhu, S. H. Sim, Y. I. Song, B. H., Hong, and J.-H. Ahn, "Wafer-Scale Synthesis and Transfer of Graphene Films", Nano Letters **10**, 490-493 (2010).

5. Y. M. Lin, C. Dimitrakopoulos, K. A. Jenkins, D. B. Farmer, H.-Y. Chiu, A. Grill, and Ph. Avouris, "100-GHz transistors from wafer-scale epitaxial graphene ," *Science* **327,** 662 (2010).
6. F. Xia, D. B. Farmer, Y. M. Lin, and Ph. Avouris, "Graphene Field-Effect Transistors with High On/Off Current Ratio and Large Transport Band Gap at Room Temperature", Nano Letters **10**, 715-718 (2010).
7. S. Bae, H. Kim, Y. Lee, S. Xu, J.-S. Park, Y. Zheng, J. Balakrishnan, T. Lei, H. R. Kim, Y. I. Song, Y. J. Kim, K. S. Kim, B. Özyilmaz, J.-H. Ahn, B. H. Hong, and S. Iijima, "Roll-to-roll production of 30-inch graphene films for transparent electrodes," Nature Nanotech. **5**, 574-578 (2010).
8. X. Du, I. Skachko, A. Barker, and E. Y. Andrei, "Approaching ballistic transport in suspended graphene", Nature Nanotech. **3**, 491-495 (2008).
9. A. H. Castro Neto, F Guinea, N. M. R. Peres, K. S. Novoselov, and A. K. Geim, "The electronic properties of graphene," Rev. Mod. Phys. **81**, 109-162 (2009).
10. G. Eda, G. Fanchini, and M. Chhowalla, "Large-area ultrathin films of reduced graphene oxide as a transparent and flexible electronic material", Nature Nanotech. **3**, 270 - 274 (2008).
11. X. Li, Y. Zhu, W Cai, M. Borysiak, B. Han, D. Chen, R. D. Piner, L. Colombo, and R.S. Ruoff, "Transfer of Large-Area Graphene Films for High-Performance Transparent Conductive Electrodes," Nano Letters **9**, 4359-4363 (2009).
12. M. Tonouchi, "Cutting-edge terahertz technology," *Nature Photon.* **1**, 97 (2007).
13. H. Choi, F. Borondics, D. A. Siegel, S. Y. Zhou, M. C. Martin, A. Lanzara, and R. A. Kaindl, "Broadband electromagnetic response and ultrafast dynamics of few-layer epitaxial graphene", Appl. Phys. Lett. **94**, 172102 (2009).
14. J. L. Tomaino, A. D. Jameson, J. W. Kevek, M. J. Paul, A. M. van der Zande, R. A. Barton, P. L. McEuen, E. D. Minot, and Yun-Shik Lee, "Terahertz Imaging and Time-Domain Spectroscopy of Large-Area Single-Layer Graphene," Opt. Express **19**, 141-146 (2011).
15. A. C. Ferrari, J. C. Meyer, V. Scardaci, C. Casiraghi, M. Lazzeri, F. Mauri, S. Piscanec, D. Jiang, K. S. Novoselov, S. Roth, and A. K. Geim, "Raman spectrum of graphene and graphene layers," Phys. Rev. Lett. **97**, 187401 (2006).
16. S. Pisana, M. Lazzeri, C. Casiraghi, K. S. Novoselov , A. K. Geim, A. C. Ferrari, and F. Mauri "Breakdown of the adiabatic Born–Oppenheimer approximation in graphene," Nat. Mater. **6**(3), 198-201 (2007).